International Journal of Computational and Experimental Science and ENgineering (IJCESEN)

Vol. 12-No.3 (2026) pp. 22-32
http://www.ijcesen.com

ISSN:2149-9144

Research Article

Mathematical modeling of rotational magneto nanofluid flow over a horizontal sheet with free stream velocity, thermal radiation, heat source and chemical reaction

Zohra Benharkat*

[1]University of Djelfa, Faculty of Sciences and Technology, Department of Common Core ST, 17000, Djelfa-Algeria

* **Corresponding AuthorEmail:** zohra.benharkat@univ-djelfa.dz- **ORCID:** 0000-0002-5247-7888

Article Info:

DOI:10.22399/ijcesen.5325
Received: 10 December 2025
Revised: 24 March 2026
Accepted: 14 May 2026

Keywords

Nanofluid
MHD
Free stream velocity
Brownian diffusivity
Thermophoresis diffusivity
Thermal radiation

Abstract:

The steady two-dimensional MHD rotational nanofluid flow with free stream velocity, thermophoresis and Brownian motion effects over a moving horizontal sheet in presence of thermal radiation, heat source and first order chemical reaction is examined. Fourth order Runge-Kutta technique of MATLAB is implement to develope the problem. The numerical results of velocity, temperature and concentration fields are presented graphically and interpreted for various flow parameters. It is determined that rising value of magnetic, heat source and thermophoresis parameters enhance the primary velocity profiles and reduce the secondary velocity profiles while an opposite behavior of the other parameters is seen. The temperature is increased for heat source, thermophoresis and Brownian motion parameters but the concentration highly increased only for thermophoresis parameter. Also, the temperature strongly varies by variations in Prandtl number.

1. Introduction

In recent times, a wide range of advanced applications of magnetohydrodynamic (MHD) employed nanofluids by combining magnetic field control with excellent thermal conductivity of nanoparticles. MHD nanofluids opened up new avenues in various research areas such as biomedicine, energy storage, plasma studies, magnetic cell insulation, electronic cooling system, optics, optical control switches, drug delivery, blood flow measurements, cancer therapeutics, nano-surgery, metallurgical processes and magneto-optical wave-length filtering systems, etc. [1, 2]

Due to these important applications, several studies have been performed on magneto nanofluids flow with heat transfer in different geometries [3-12]. On the other hand, the heat transfer and MHD nanofluids flow problems over a stretching surface are mostly studied by numerous researchers owing to its high applicability in medical and manufacturing processes [1]. In connection to these, steady two-dimensional flow is one of the problems that acquired much attention. For example, S.S. Ghadikolaei et al. [13] analyzed the influence of a magnetic field on stagnation-point flow and heat transfer of hybrid nanofluid towards a horizontal linearly stretching surface using numerical method of Runge-Kutta Fehlberg. M. Asif Zahoor Raja et al. [14] examined the entropy generation of Darcy-Forchheimer nanofluid flow along a horizontal stretching sheet with second order slip, thermal radiation and heat sink/source using artificial neural network. The opposing hybrid nanofluid flow was investigated by A'isyah Jaafar et al. [15] under an exponentially vertical stretching/shrinking surface immersed in a porous medium in the presence of heat source and slip conditions. Muhammad Ramzan et al. [16] explored the flow of Carreau trihybrid nanoliquid past a horizontal stretching sheet embedded in a porous medium with thermal radiation and heat source/sink effects. Hanifa Hanif et al. [17] analyzed the effects of the entropy generation of magnetized ferrofluid over a vertical flat surface with variable wall temperature in the presence of heat generation by applying an implicit finite difference, and employed the Crank-Nicolson method to investigate the unsteady hybrid nanofluid flow over a horizontal plate with Joule heating, viscous dissipation, suction and thermal slip [18].

Moreover, combined heat and mass transfer problems are the other kind of field of interest in

analyzing MHD nanofluids flow. Many geometries have attracted attention by researchers, some are; sphere [19], wedge surface [20-23], circular cylinder [24-26], disk surface [27-31], slender needle [32] and curved surface [33].

Also, significant review papers have been done to study magneto nanofluids flowing, heat and mass transfer past a flat surface with various situations. A number of studies have considered the steady two-dimensional boundary layer flow, like Nemat Dalir et al. [34] presenting the forced convection of a non-Newtonian Jeffrey nanofluid over a linearly stretching impermeable isothermal sheet with entropy generation and viscous dissipation, Maria Imtiaz et al. [35] considering an exponentially stretching sheet in the presence of viscous dissipation and radiation effects, Yahaya Shagaiya Daniel et al. [36] proposing the effects of thermal radiation, viscous dissipation and Joule heating over a permeable linear stretching sheet and S. Abdul Gaffar et al. [37] using the non-Newtonian Jeffrey's model along a semi-infinite vertical plate. The unsteady two-dimensional boundary layer flow past an inclined permable stretching sheet was investigated by Shalini Jain et al. [38] in the presence of suction/injection, non-linear heat source, non-linear radiation and n order chemical reaction. D.V. Krishna Prasad et al. [39] discussed the influence of thermal diffusion on unsteady two-dimensional mixed convection Casson fluid flow past an accelerated vertically inclined wavy plate embedded in a darcian porous medium in the presence of heat absorption, thermal radiation and chemical reaction. M. Ijaz Khan et al. [40] analyzed the effect of entropy optimization and Bejan number in steady two-dimensional chemically reactive flow of Prandtl-Eyring nanofluid over a linearly stretching surface with activation energy, non-linear radiation and Joule heating. Irfan Haider et al. [41] applied finite element method to investigate the role of hybrid nanostructures on the thermos-physical properties in Williamson nanofluid towards horizontal stretched surface with porous medium under non-Fourier's heat conduction and non-Fourier's Fick's law. The homotopy analysis method was employed by Abdullah Dawar et al. [42] to study the steady two-dimensional stagnation point flow of non-Newtonian fluid past a flat plate in the presence of solar radiation. The effect of chemical reaction on steady three dimensional rotating flow above extending surface horizontally was examined by Aziz Ullah Awan et al. [43] using hybrid nanofluid, Kashif Ali et al. [44] using zirconium oxide and single wall-carbon nanotubes and by Fuzhang Wang et al. [45] using non-Newtonian Maxwell nanofluid through a porous medium with Brownian and thermophoresis diffusivity, thermal radiation and heat source/sink. Fuzhang Wang et al. [46] considered the steady three dimensional flow via stretching sheet with thermal radiation and slip conditions. In another work, Aaqib Majeed et al. [47] studied the steady three dimensional flow of non-Newtonian Oldroyd-B nanofluid via exponentially expanding surface by taking into account thermal radiation, slip conditions, n order chemical reaction and heat generation. The exact solutions of the unsteady blood flow containing gold nanoparticles between two parallel flat plates through a porous medium were developed by Shafiq Ahmad et al. [48] utilizing Fick's and Fourier's laws approach. Considering thermal radiation, thermophoresis, Brownian motion and motile microorganisms, the problem of three-dimensional bioconvection flow of rotating hybrid nanofluid between two horizontal plates was published by Mubashar Arshad [49] .

In modern epoch, to discuss the MHD effect on convection heat and mass transfer characteristics, Artificial neural networks are frequently used in several works, including M. Elayarani et al. [50] for unsteady bio-convection flow of Carreau nanofluid incorporating gyrotactic micro-organisms over a slendering stretching sheet with thermal radiation and multiple slip conditions, Muhammad Asif Zahoor Raja et al. [51] for oblique stagnated flow of steady bioconvection Casson nanofluid along a stretched sheet involving Lorentz force interaction and gyrotactic microorganisms with partial slip and Newtonian heating, Muhammad Shoaib et al. [52] for Casson nanofluid flow over a nonlinear slanted extending surface in a Forchheimer permeable medium with slip velocity, heat source, thermal radiation and chemical reaction, Anum Shafiq et al. [53] for bioconvective flow of thixotropic nanofluid through a vertical surface with Brownian motion, thermophoresis, convective condition, and radiation influences, Amna et al. [54] for three-dimensional non-Newtonian Darcy-Forchheimer flow of Casson nanofluid past a stretching surface in a porous medium with Hall and ion slip forces, Pradeep Kaswan et al. [55] for cross-bioconvection flow on a stretching surface including gyrotactic microorganisms under thermal radiation, Zeeshan Ikram Butt et al. [56] for Casson nanofluid flow along a permeable extended surface in a porous medium with different slips, and Zulqurnain Sabir et al. [57] for steady three dimensional rotating Maxwell nanofluid flow over a linear and exponential stretching sheets with varying thermal conductivity, heat source/sink and reactive species.

As results, the problem of convective heat and mass transfer for the steady two-dimensional MHD flow past a moving horizontal sheet in a nano rotational fluid with free stream velocity effect has unexplored in the literature. So, the objective of this study is to

extend the work of H.S. Takhar et al. [58] to consider nanofluid, to neglect the Hall effects, and to include the thermal radiation, heat source and first order chemical reaction. This work was developed by using the similarity transformations and the fourth order Runge-Kutta technique of MATLAB. The numerical results of velocity, temperature and concentration fields are presented graphically and interpreted for various flow parameters.

2. Mathematical formulation

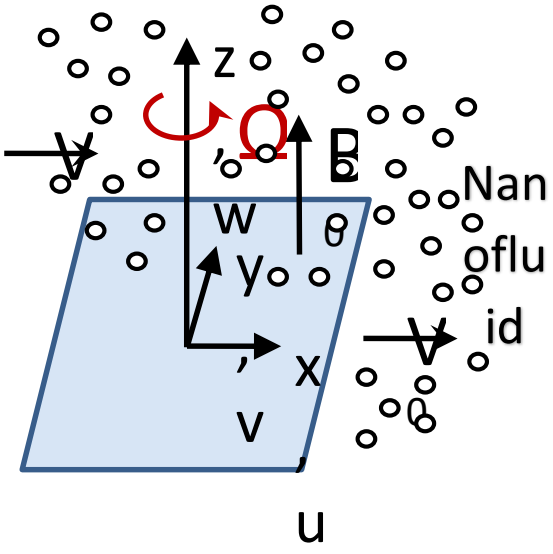

Figure 1. *Problem geometry.*

A steady flow of an incompressible, viscous and electrically conducting nanofluid past a moving horizontal sheet. Fig. 1 represents the physical configuration and Cartesian coordinate system, where the plate is aligned through the *xy*-plane and *z*-axis is normal to it. Also, this plate is considered infinite in *y*-direction, then the physical quantities will be depend on x and z only. At the wall, the temperature T and the concentration C take constant values T_w and C_w respectively. Far away from the sheet, the ambient temperature and concentration are T_∞ and C_∞ respectively. A uniform magnetic field of intensity B_0 is applied in the *z*-direction and in the positive *x*-direction the plate moves uniformly with velocity V_0 in the presence of a uniform free stream of velocity V. The nanofluid is rotating with angular velocity Ω about the *z*-axis. We consider that the nanoparticles have a uniform very small size and shape which are in thermal equilibrium with the fluid phase. In addition, both magnetic and electric field is assumed very less while magnetic Reynolds number of the flow is small. Therefore, Hall current and ionslip effects are also neglected. The heat and mass transport properties is computed by using the thermal radiation, heat source, first order chemical reaction, thermophoresis and Brownian diffusivity.

Taking into account the model of H.S. Takhar et al. [58] and the preceding assumptions with the Boussinesq approximation, the continuity, momentum, energy and concentration equations can be given as [34-36]:

$$\frac{\partial u}{\partial x}+\frac{\partial w}{\partial z}=0 \tag{1}$$

$$u\frac{\partial u}{\partial x}+w\frac{\partial u}{\partial z}-2\Omega v=-\frac{1}{\rho}\frac{\partial p}{\partial x}+\nu\frac{\partial^2 u}{\partial z^2} +g\beta(T-T_\infty)+g\beta^*(C-C_\infty)-\left(\frac{\sigma B_0^2}{\rho}\right)u \tag{2}$$

$$u\frac{\partial v}{\partial x}+w\frac{\partial v}{\partial z}+2\Omega u=-\frac{1}{\rho}\frac{\partial p}{\partial y}+\nu\frac{\partial^2 v}{\partial z^2}-\left(\frac{\sigma B_0^2}{\rho}\right)v \tag{3}$$

$$u\frac{\partial T}{\partial x}+w\frac{\partial T}{\partial z}=\frac{k}{\rho c_p}\frac{\partial^2 T}{\partial z^2}+\tau\left[D_B\frac{\partial C}{\partial z}\frac{\partial T}{\partial z}+\frac{D_T}{T_\infty}\left(\frac{\partial T}{\partial z}\right)^2\right] +\frac{16\sigma^* T_\infty^3}{3k^*\rho c_p}\frac{\partial^2 T}{\partial z^2}+\frac{Q}{\rho c_p}(T-T_\infty) \tag{4}$$

$$u\frac{\partial C}{\partial x}+w\frac{\partial C}{\partial z}=D_B\frac{\partial^2 C}{\partial z^2}+\frac{D_T}{T_\infty}\frac{\partial^2 T}{\partial z^2}-K_r(C-C_\infty) \tag{5}$$

where, the kinematics viscosity is ν, the fluid density is ρ, β and β^* are the thermal and mass diffusions coefficients, c_p is the fluid specific heat at constant pressure, K_r is the rate of reaction constant, Q is the additional heat source, k^* is the mean absorption coefficient, σ^* is the Stefan-Boltzman constant, D_B and D_T are the Brownian diffusion and the thermophoretic diffusion coefficients, respectively.
Neglecting the Hall current, the gradients of pressure far away from the sheet take the following forms [58]:

$$-\frac{1}{\rho}\frac{\partial p}{\partial x}=\left(\frac{\sigma B_0^2}{\rho}\right)V, \qquad -\frac{1}{\rho}\frac{\partial p}{\partial y}=2\Omega V \tag{6}$$

The boundary conditions are

$$u=V_0, v=0, w=0, T=T_w, C=C_w \ \ at \ \ z=0,\\ u=V, \ v=0, \ T=T_\infty, \ C=C_\infty \ \ as \ \ z\to\infty \tag{7}$$

The used similarity transformations are

$$\eta=\sqrt{\frac{\Omega}{\nu}}z, \ u=\Omega x F_1', \ v=\Omega x F_2, \quad w=-\sqrt{\Omega\nu}F_1,\\ F_3=\frac{(T-T_\infty)}{(T_w-T_\infty)}, \ F_4=\frac{(C-C_\infty)}{(C_w-C_\infty)}, \quad \chi=\frac{\Omega x}{U}, U=V_0+V,\\ \delta=\frac{V_0}{V} \tag{8}$$

Further, χ and δ represent the dimensionless quantities of the Coriolis force and velocity ratio at the wall and which called Coriolis and wall velocity parameters, respectively.
The resulting similarity equations with boundary conditions can be taken the form as

$$F_1'''+F_1F_1''-F_1'^2+2F_2+GrF_3+GmF_4 +M\left[\frac{(1-\delta)}{\chi}-F_1'\right]=0 \tag{9}$$

$$F_2'' + F_1F_2' - F_1'F_2 - 2F_1' - MF_2 + \frac{2(1-\delta)}{\chi} = 0 \quad (10)$$

$$F_3'' + \frac{1}{1+\frac{4}{3}R}\left[PrF_1F_3' + N_bF_3'F_4' + N_tF_3'^2 + BPrF_3\right] = 0 \quad (11)$$

$$F_4'' + Sc\frac{N_t}{N_b}F_3'' + ScF_1F_4' - \gamma ScF_4 = 0 \quad (12)$$

and

$$F_1'(0) = \frac{\delta}{\chi}, F_1(0) = 0, F_2(0) = 0, F_3(0) = 1, F_4(0) = 1,$$
$$F_1'(\infty) = \frac{1-\delta}{\chi},\ F_2(\infty) = 0,\ F_3(\infty) = 0,\ F_4(\infty) = 0 \quad (13)$$

where $M,\ Gr,\ Gm, R, Pr, B, N_t,\ N_b,\ Sc,\ \gamma$ are the magnetic parameter, thermal Grashof number, mass Grashof number, radiation parameter, Prandtl number, heat source parameter, thermophoresis parameter, Brownian motion parameter, Schmidt number and chemical reaction parameter, respectively, which are defined as:

$$M = \frac{\sigma B_0^2}{\rho\Omega},\ \ r = \frac{g\beta(T_w - T_\infty)}{\Omega^2 x},\ \ Gm = \frac{g\beta^*(C_w - C_\infty)}{\Omega^2 x},$$
$$R = \frac{4\sigma^* T_\infty^3}{KK^*},\ \ Pr = \frac{\rho\nu c_p}{k},\ B = \frac{Q}{\rho c_p \Omega},$$
$$N_t = \frac{\tau\rho c_p D_T(T_w - T_\infty)}{T_\infty k},\quad N_b = \frac{\tau\rho c_p D_B(C_w - C_\infty)}{k},$$
$$Sc = \frac{\nu}{D_B},\ \ \gamma = \frac{K_r}{\Omega} \quad (14)$$

3. Solution methodology

The fourth order Runge Kutta scheme is used to solve numerically the governing nonlinear ordinary differential equations (9-12) and associated boundary conditions (13). Let us substitute

$$y_1 = F_1,\quad y_2 = F_1',\quad y_3 = F_1'',$$
$$-y_1y_3 + y_2^2 - 2y_4 - Gry_6 - Gmy_8 - M\left(\frac{(1-\delta)}{\chi} - y_2\right) = F_1'''$$
$$y_4 = F_2,\quad y_5 = F_2',$$
$$-y_1y_5 + 2\,y_2 + y_2y_4 + My_4 - \frac{2(1-\delta)}{\chi} = F_2''$$
$$y_6 = F_3,\quad y_7 = F_3',$$
$$\frac{1}{1+\frac{4}{3}R}(-Pry_1y_7 - N_by_7y_9 - N_ty_7^2 - BPry_6) = F_3''$$
$$y_8 = F_4,\quad y_9 = F_4',$$
$$Sc\left(-\frac{N_t}{N_b}y_6 - y_1y_9 + \gamma y_8\right) = F_4'' \quad (15)$$

with

$$y_2(0) = \frac{\delta}{\chi},\quad y_1(0) = 0,\quad y_4(0) = 0,\quad y_6(0) = 1,\quad y_8(0) = 1$$
$$y_2(\infty) = \frac{1-\delta}{\chi}, y_4(\infty) = 0,\ y_6(\infty) = 0, y_8(\infty) = 0 \quad (16)$$

The above equations are integrated by executing the code in MATLAB to acquire numerical results, and subsequently analyze the graphical outcomes.

4. Results and Discussions

The graphical outcomes are gained for various parameters such as magnetic parameter M, radiation parameter R, heat source parameter B, thermophoresis and Brownian motion parameters, N_t and N_b, and chemical reaction parameter γ. The velocity, temperature and concentration profiles are analyzed for *Pr*=0.71, *Sc*=1, *Gr*=0.3, *Gm*=0.3, δ =0.25 and χ =0.75.

Figs. 2 and 3 show the velocity profiles for various values of Pr. It can be seen that the increase of Prandtl number causes the decrease of $F_1'(\eta)$ and the increase of $F_2(\eta)$. Figs. 4-15 exhibit the influences of different parameters on the dimensionless velocity profiles $F_1'(\eta)$ and $F_2(\eta)$. The effects of magnetic parameter M are shown in Figs. 4 and 5, which illustrated that an increase in magnetic field increases the primary u-velocity $F_1'(\eta)$ while reduce the secondary v-velocity $F_2(\eta)$. Lorentz force, which is created by the magnetic field, acts as a retarding force that leads to decrease the secondary velocity $F_2(\eta)$. In contrast, an accelerating current due to the induction of an electric field can be created perpendicular to the secondary direction and causes an increase in the primary velocity $F_1'(\eta)$. It is observed that cross flux produced due to impacts of Coriolis forces. Influence of radiation parameter R on the velocity field can be seen in Figs. 6 and 7. This parameter decreases the primary velocity profile $F_1'(\eta)$ and increases the secondary velocity profile $F_2(\eta)$. A larger radiation parameter is associated with an increase in the rate of heat transfer which consequently increases the ratio of kinetic energy and flow velocity in the secondary direction. The behavior of heat source variable on $F_1'(\eta)$ and $F_2(\eta)$ is displayed in Figs. 8 and 9. An increase in the heat source parameter B increases the velocity profile $F_1'(\eta)$ but reduces the secondary velocity profile $F_2(\eta)$. The impact of thermophoresis parameter N_t is depicted in Figs. 10 and 11. We see that this parameter has an increasing effect on velocity profile $F_1'(\eta)$ but reduces the secondary velocity $F_2(\eta)$. A reverse trend is shown for Brownian motion parameter N_b (see Figs. 12 and 13) and chemical reaction parameter γ (see Figs. 14 and 15). The Brownian motion generates random motion of particles and micro-mixing which rises the collisions between particles hence primary velocity $F_1'(\eta)$ reduces whereas secondary velocity $F_2(\eta)$ increases.

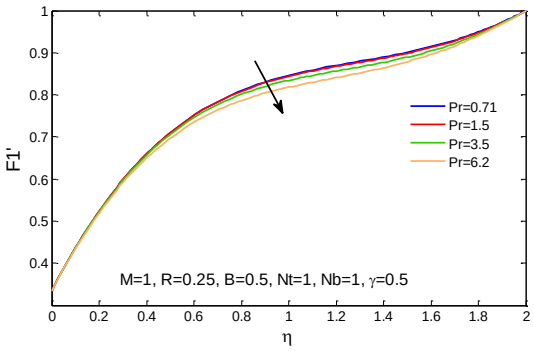

Figure 2. *Influence of Pr on u-velocity profiles.*

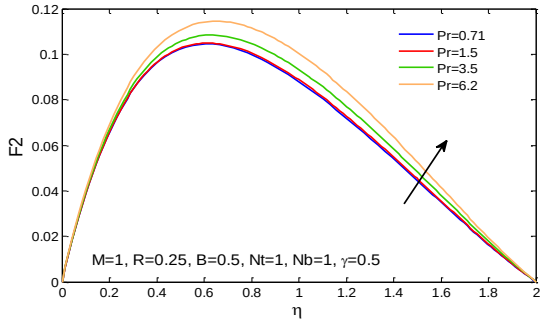

Figure 3. *Influence of Pr on v-velocity profiles.*

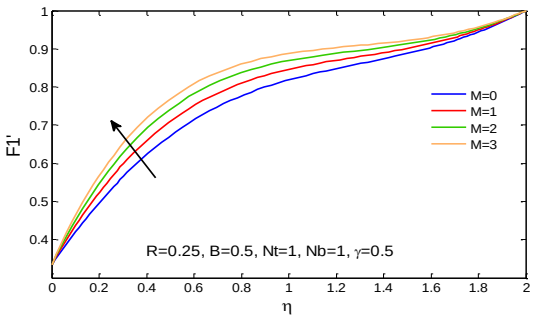

Figure 4. *Influence of M on u-velocity profiles.*

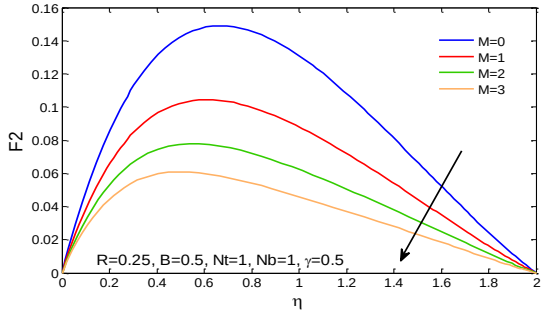

Figure 5. *Influence of M on v-velocity profiles.*

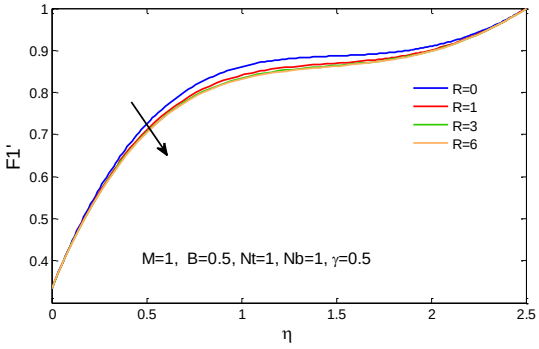

Figure 6. *Influence of R on u-velocity profiles.*

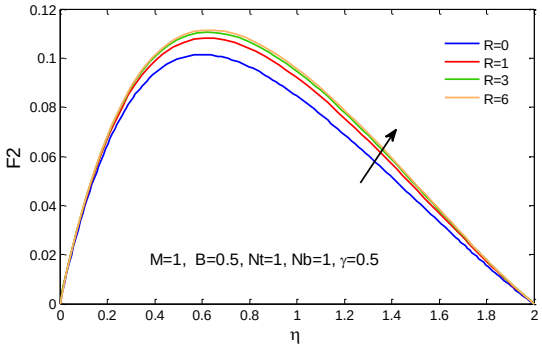

Figure 7. *Influence of R on v-velocity profiles.*

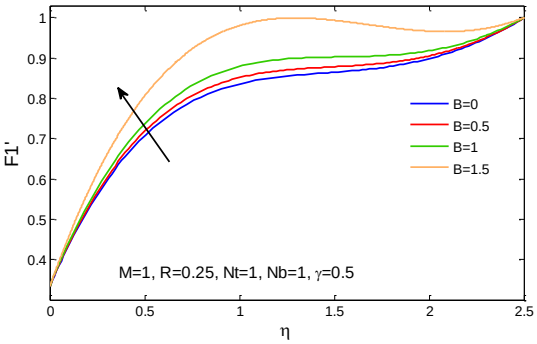

Figure 8. *Influence of B on u-velocity profiles.*

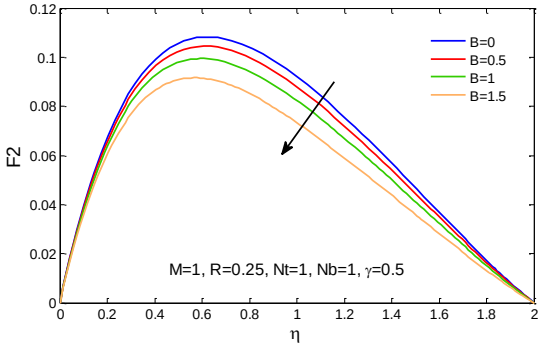

Figure 9. *Influence of B on v-velocity profiles.*

The effects of different parameters on the temperature profiles $F_3(\eta)$ are displayed in Figs. 16-22. The effect of Pr is displayed in Fig. 16. For $\eta < 0.5$, a slight increase is seen in temperature with increasing Pr values and a substantial reduction in the fluid temperature is seen for $\eta > 0.5$.

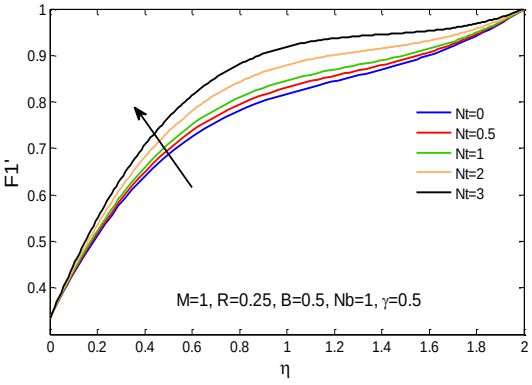

Figure 10. *Influence of N_t on u-velocity profiles.*

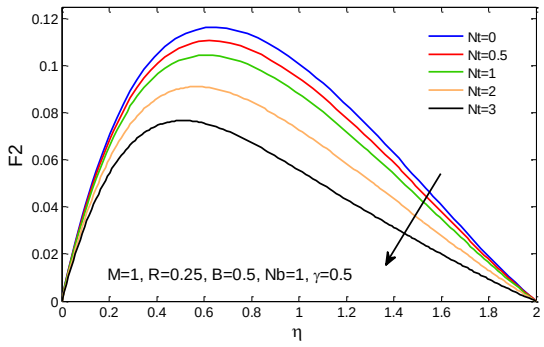

Figure 11. *Influence of N_t on v-velocity profiles.*

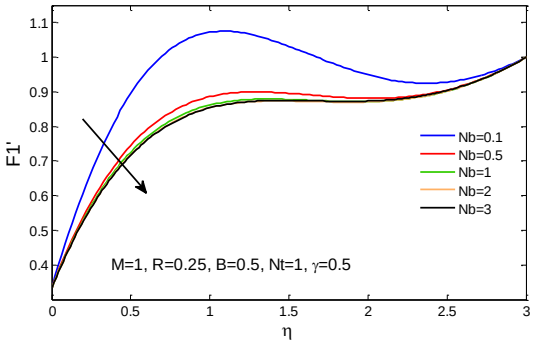

Figure 12. *Influence of N_b on u-velocity profiles.*

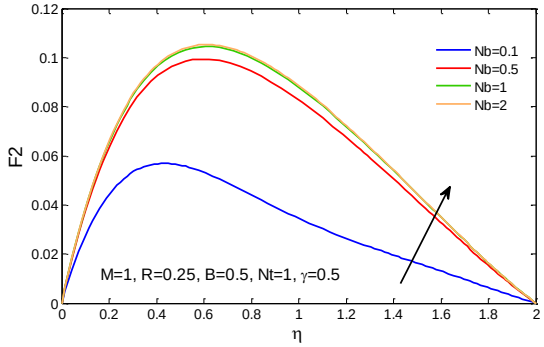

Figure 13. *Influence of N_b on v-velocity profiles.*

It is shown in Fig. 17 that the increase of magnetic parameter M slightly reduces the temperature. An increase in the magnetic field, increases the Lorentz force resisting the velocity profile and causes a reduction in the electrically conducting nanofluid which gives way to decrease the temperature. Decreasing in temperature distribution is observed for increasing radiation parameter R, as shown in Fig. 18. According to Eq. (14), temperature is inversely proportional to the radiation parameter, thus an increase in R causes the decrease in $F_3(\eta)$. From Fig. 19, an increase of heat source parameter B causes a high enhancement in temperature. As larger values of B enhances the heat flux therefore temperature increases. It is seen in Figs. 20 and 21 that the temperature is an increasing function of the thermophoresis parameter N_t and Brownian motion parameter N_b, respectively. Basing on Eq. (14), the temperature is directly proportional to the thermophoresis and Brownian motion parameters, thus an increase in N_t and N_b is equivalent to enhancement in temperature. However, the Brownian motion enhances the thermal conductivity of the nanofluid by generating micro-mixing which in effect causes the increase of temperature. In Fig. 22, the effect of chemical reaction parameter γ on $F_3(\eta)$ is illustrated. It is observed that an intensification in γ leads to a slight decrease in the temperature.

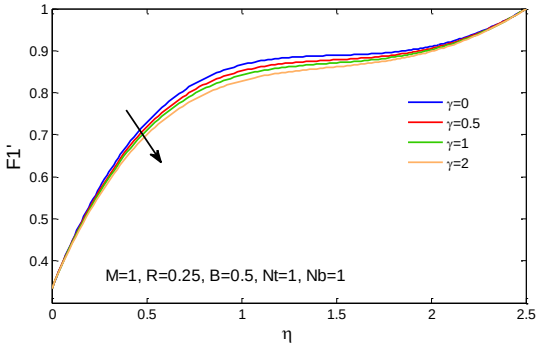

Figure 14. *Influence of γ on u-velocity profiles.*

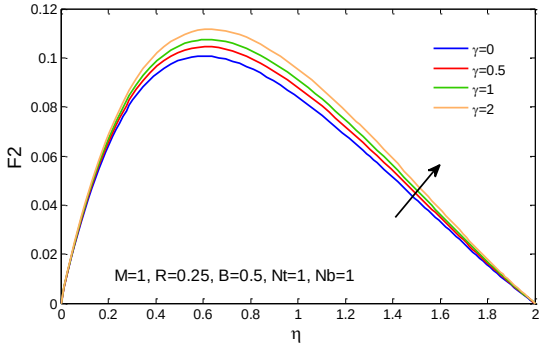

Figure 15. *Influence of γ on v-velocity profiles.*

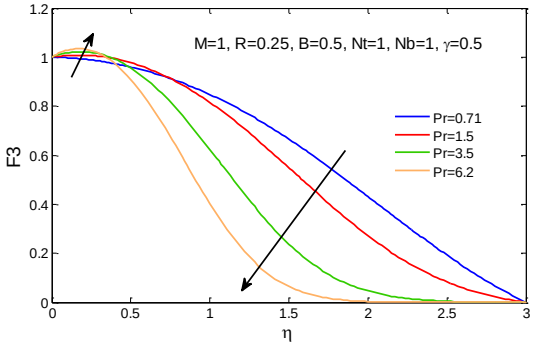

Figure 16. *Influence of Pr on temperature profiles.*

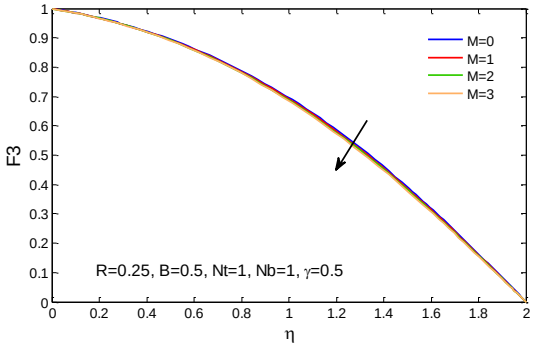

Figure 17. *Influence of M on temperature profiles.*

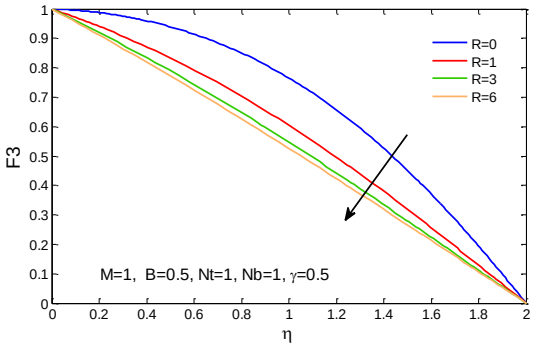

Figure 18. *Influence of R on temperature profiles.*

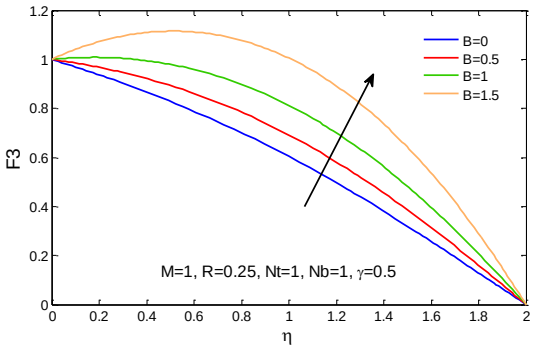

Figure 19. *Influence of B on temperature profiles.*

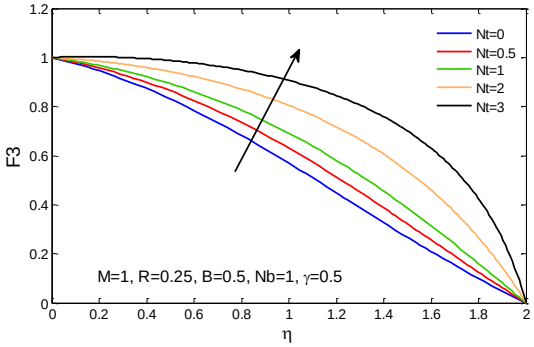

Figure 20. *Influence of N_t on temperature profiles.*

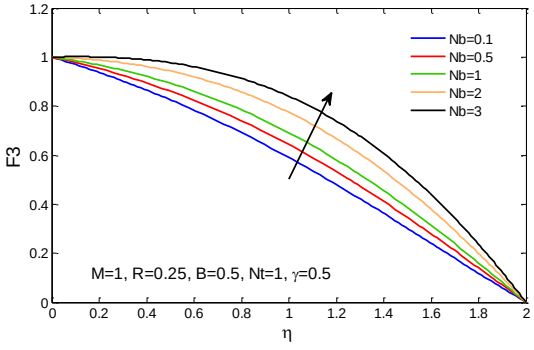

Figure 21. *Influence of N_b on temperature profiles.*

Figs. 23-30 describe the effects of above parameters on the concentration profiles $F_4(\eta)$. In general, enhancing values of all above parameters decrease the concentration distribution except the thermophoresis parameter N_t. Figs. 23 and 24 present the concentration profiles $F_4(\eta)$ for various values of Prandtl and Schmidt numbers respectively. With increasing Pr values, the concentration decreased, as seen in Fig. 23.

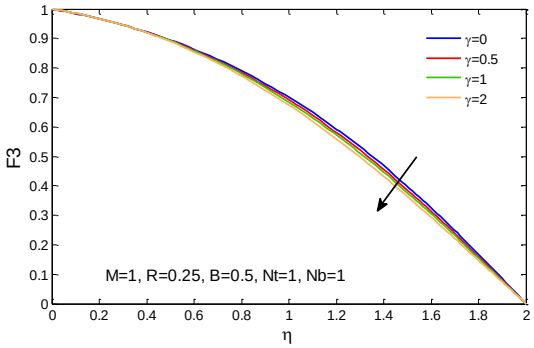

Figure 22. *Influence of γ on temperature profiles.*

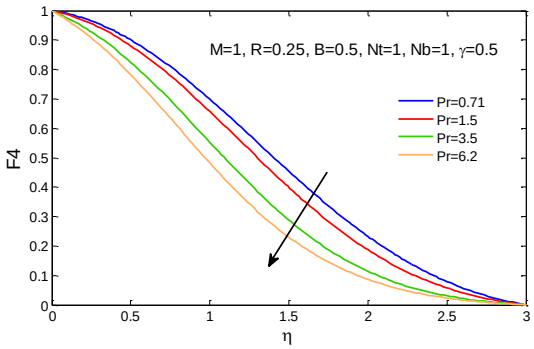

Figure 23. *Influence of Pr on concentration profiles.*

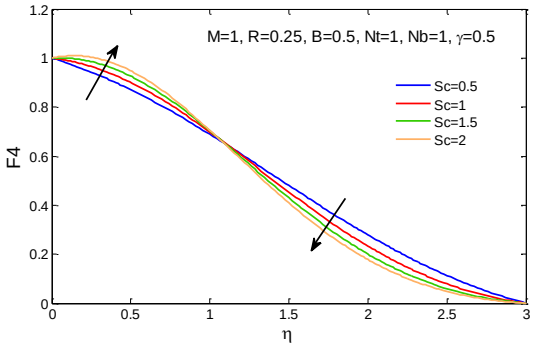

Figure 24. *Influence of Sc on concentration profiles.*

Fig. 24 shows that for $Sc < 1$, the concentration profiles increase and vice versa for $Sc > 1$. The magnetic parameter M does not considerably affect the concentration, as seen in Fig. 25. It is because the slight decrease of nanoparticles volume fraction due to the lower fluid motion caused by the cross flux.

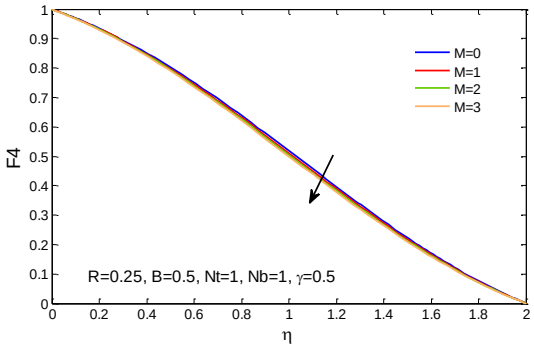

Figure 25. *Influence of M on concentration profiles.*

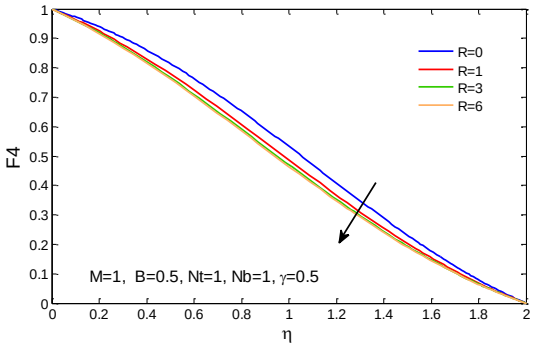

Figure 26. *Influence of R on concentration profiles.*

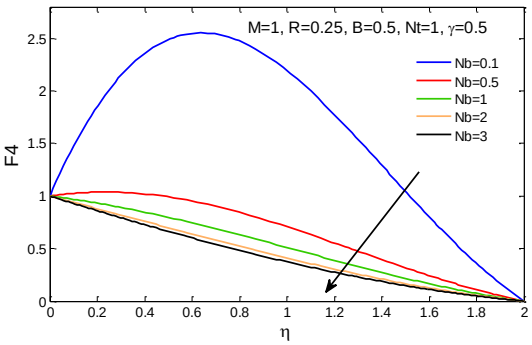

Figure 29. *Influence of N_b on concentration profiles.*

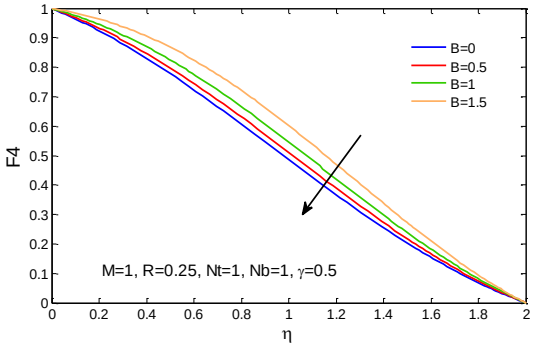

Figure 27. *Influence of B on concentration profiles.*

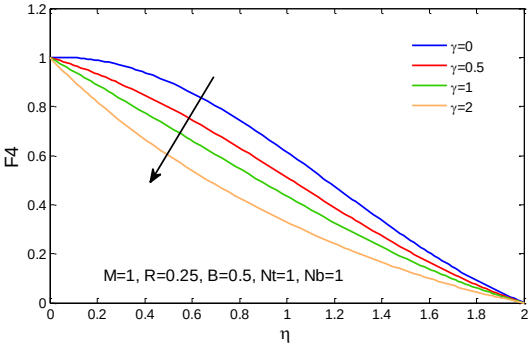

Figure 30. *Influence of γ on concentration profiles.*

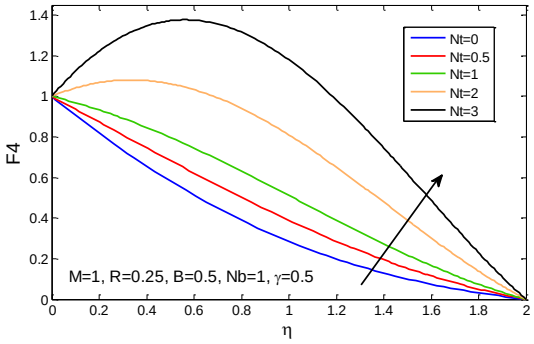

Figure 28. *Influence of N_t on concentration profiles.*

When radiation and heat source parameters increase in Figs. 26 and 27, the temperature gradients increases and consequently the particles move away from hotter areas, leading to decrease the concentration. Conversely, the thermophoresis parameter N_t highly increases the concentration, as illustrated in Fig. 28. The thermophoresis parameter enhances diffusion and causes a more uniform dispersion of particles, causing higher concentration distribution in the fluid. From Fig. 29, Brownian motion parameter N_b diminishes the concentration profiles $F_4(\eta)$. The reason is that the Brownian motion enhances the thermal conductivity and thermophoretic force of the nanofluid which tends to move the nanoparticles from hot to cold region and results the decrease of concentration. For increasing γ, the chemical species consumption increases more effectively, causing a fall in concentration field, according to Fig. 30.

5. Conclusion

In this investigation, the steady two-dimensional MHD flow past a moving horizontal sheet in a nano rotational fluid is analyzed by incorporating the free stream velocity, thermophoresis and Brownian motion effects in presence of thermal radiation, heat source and first order chemical reaction. Similarity transformations are used to obtain the coupled ordinary differential equations which are solved with the fourth order Runge-Kutta technique of MATLAB. The numerical results of velocity, temperature and concentration profiles are interpreted for various parameters. The obtained results are as follows:

- With the increase of magnetic, heat source and thermophoresis parameters, primary velocity enhances while secondary velocity reduces. However, opposite behavior of the radiation, Brownian motion and chemical reaction parameters is seen on the velocity profiles.
- The temperature is reduced for magnetic and chemical reaction parameters but increased for heat source, thermophoresis and Brownian motion parameters.
- The concentration field is decreased with rising value of all parameters but highly increased with thermophoresis parameter.
- The temperature is considerably reduced with increasing Prandtl number.

Author Statements:

- **Ethical approval:** The conducted research is not related to either human or animal use.
- **Conflict of interest:** The authors declare that they have no known competing financial interests or personal relationships that could have appeared to influence the work reported in this paper
- **Acknowledgement:** The authors declare that they have nobody or no-company to acknowledge.
- **Author contributions:** The authors declare that they have equal right on this paper.
- **Funding information:** The authors declare that there is no funding to be acknowledged.
- **Data availability statement:** The data that support the findings of this study are available on request from the corresponding author. The data are not publicly available due to privacy or ethical restrictions.
- **Use of AI Tools:** The author(s) declare that no generative AI or AI-assisted technologies were used in the writing process of this manuscript.

References

1. Sheikholeslami, M., Hatami, M., Ganji, D.D. (2014). Nanofluid flow and heat transfer in a rotating system in the presence of amagnetic field. *Journal of Molecular Liquids.* (190): 112-120.
2. Andaç B.Ç. (2022). Prediction of viscous dissipation effects on magnetohydrodynamic heat transfer flow of copper-poly vinyl alcohol Jeffrey nanofluid through a stretchable surface using artificial neural network with Bayesian Regularization. *Chemical Thermodynamics and Thermal Analysis*. (6): 100056.
3. Ammara, M., Aneela, Z., Muhammad Asif, Z.R. (2018). Intelligent computing to analyze the dynamics of Magnetohydro-dynamic flow over stretchable rotating disk model. *Applied Soft Computing*. (67): 8-28.
4. Mohammad, M.A., Alim, M.A. , Ahmed, S.S. (2019), Oriented magnetic field effect on mixed convective flow of nanofluid in a grooved channel with internal rotating cylindrical heat source. *International Journal of Mechanical Sciences*. (151): 385-409.
5. Ijaz Khan, M., Faqir S., Hayat, T., Alsaedi, A. (2019). Transportation of CNTs based nanomaterial flow confined between two coaxially rotating disks with entropy generation. *Physica A*. (527): 121154.
6. Awais, M., Bibi, M., Zahoor Raja, M. A., Awan, S.E., Malik, M.Y. (2021), Intelligent numerical computing paradigm for heat transfer effects in a Bodewadt flow. *Surfaces and Interfaces*. (26): 101321.
7. Hossain, R., Jahid Hasan, M., Azad, A.K., Rahman M.M. (2022). Numerical study of low Reynolds number effect on MHD mixed convection using CNT-oil nanofluid with radiation. *Results in Engineering*. (14): 100446.
8. Shah, N.A., Asogwa, K.K., Mahsud, Y., Lee, S., Kang, S., Chung, J. D., Ishtiaq, A.M. (2022). Effect of generalized thermal transport on MHD free convection flows of nanofluids: A generalized Atangana-Baleanu derivative model. *Case Studies in Thermal Engineering*. (40): 102480.
9. Rehman, R., Wahab, H.A., Khan, U. (2022). Heat transfer analysis and entropy generation in the nanofluids composed by Aluminum and γ^{-} Aluminum oxides nanoparticles. *Case Studies in Thermal Engineering*. (31): 101812.
10. Jalili, B., Roshani, H., Jalili, P., Jalili, M., Pasha, P., Ganji D.D. (2023). *Case Studies in Thermal Engineering*. (45): 102961.
11. Hanif, H., Jamshed, W., Devi S.U., Eid, M.R., Shafie, S., Ibrahim, R.W., Mohd Nasir, N.A.A., Abd-Elmonem, A., El Din S.M. (2023) . Thermal description and entropy evaluation of magnetized hybrid nanofluid with variable viscosity via Crank-Nicolson method. *Case Studies in Thermal Engineering*. (47): 103132.
12. Hayat, T., Rehman, W., Ahmed, B., Momani, S. (2023). Peristalsis for MHD hybrid nanomaterial through asymmetric channel. *Alexandria Engineering Journal*. (78): 65-73.
13. Ghadikolaei, S.S., Yassari, M., Sadeghi, H., Hosseinzadeh, K., Ganji, D.D. (2017). Investigation on thermophysical properties of Tio2–Cu/H2O hybrid nanofluid transport dependent on shape factor in MHD stagnation point flow. *Powder Technology*. (322): 428-438.
14. Asif Zahoor Raja, M., Shoaib, M., Tabassum, R., Khan, N.M., Kehili, S., Bafakeeh, O.T. (2022). Stochastic numerical computing for entropy optimized of Darcy-Forchheimer nanofluid flow: Levenberg Marquardt Algorithm. *Chemical Physics Letters*. (807): 140070
15. Jaafar, A., Jamaludin, A., Mohd Nasir, N.A.A., Nazar, R., Pop, I. (2023) . MHD opposing flow of Cu -TiO2 hybrid nanofluid under an exponentially stretching/shrinking surface embedded in porous media with heat source and slip impacts. *Results in Engineering*. (17): 101005.
16. Ramzan, M., Ali, F., Akkurt, N., Saeed, A., Kumam, P., Galal, A.M. (2023). Computational assesment of Carreau ternary hybrid nanofluid influenced by MHD flow for entropy generation. *Journal of Magnetism and Magnetic Materials*. (567): 170353.
17. Hanif, H., Shafie, S., Rawi, N.A., Mohd Kasim, A.R. (2023). Entropy analysis of magnetized ferrofluid over a vertical flat surface with variable heating. *Alexandria Engineering Journal*. (65): 897-908.
18. Hanifa, H., Jamshed, W., Eid, M.R., Devi S, S.U., Ibrahim, R.W., Shafie, S., Raezah, A.A., El Din, S.M. (2023). Numerical Crank-Nicolson methodology analysis for hybridity aluminium alloy nanofluid flowing based-water via stretchable

horizontal plate with thermal resistive effect. *Case Studies in Thermal Engineering*. (42): 102707.
19. Gaffar, S.A. , Prasad, R.V., Reddy, E. K. (2015). Bég, O.A. Thermal radiation and heat generation/absorption effects on viscoelastic double-diffusive convection from an isothermal sphere in porous media. *Ain Shams Engineering Journal*. (6): 1009-1030.
20. Abdul Gaffar, S., Ramachandra Prasad, V., Keshava Reddy, E. (2017). Mixed convection boundary layer flows of a non-Newtonian Jeffrey's fluid from a non-isothermal wedge. *Ain Shams Engineering Journal*. (8): 145-162.
21. Goqo, S.P., Oloniiju, S.D., Mondal, H., Sibanda, P., Motsa, S.S. (2018). Entropy generation in MHD radiative viscous nanofluid flow over a porous wedge using the bivariate spectral quasi-linearization method. *Case Studies in Thermal Engineering*. (12): 774-788.
22. Khan, U., Shafiq, A., Zaib, A., Wakif, A., Baleanu, D. (2020). Numerical exploration of MHD falkner-skansutter by nanofluid flow by utilizing an advanced non-homogeneous two-phase nanofluid model and non-fourier heat-flux theory. *Alexandria Engineering Journal*. (59): 4851-4864.
23. Butt, Z.I., Ahmad, I., Shoaib, M., Ilyas, H., Asif Zahoor Raja, M. (2023). A novel design of inverse multiquadric radial basis neural networks to analyze MHD nanofluid boundary layer flow past a wedge embedded in a porous medium under the influence of radiation and viscous effects. *International Communications in Heat and Mass Transfer*. (140): 106516.
24. Irfan, M., Khan, M., Khan, W.A., Ayaz, M. (2018). Modern development on the features of magnetic field and heat sink/source in Maxwell nanofluid subject to convective heat transport. *Physics Letters A*. (382): 1992-2002.
25. Qureshi, Z.A., Bilal, S., Khan, U., Akgül, A., Sultana, M., Botmart, T., Zahran, H.Y., Yahia, I.S. (2022). Mathematical analysis about influence of Lorentz force and interfacial nano layers on nanofluids flow through orthogonal porous surfaces with injection of SWCNTs. *Alexandria Engineering Journal*. (61): 12925-12941.
26. Asif Zahoor Raja, M., Nisar, K.S., Shoaib, M., Abukhaled, M., Riaz, A. (2023). Intelligent computing for MHD radiative Von Kármán Casson nanofluid along Darcy-Fochheimer medium with activation energy. *heliyon*. 20911.
27. Uddin, I., Ullah, I., Asif Zahoor Raja, M., Shoaib, M., Islam, S., Muhammad, T. (2021). Design of intelligent computing networks for numerical treatment of thin film flow of Maxwell nanofluid over a stretched and rotating surface. *Surfaces and Interfaces*. (24): 101107.
28. Shoaib, M., Zubair, G., Nisar, K.S., Asif Zahoor Raja, M., Khan, I., Punith Gowda, R.J., Prasannakumara, B.C. (2021). Ohmic heating effects and entropy generation for nanofluidic system of Ree-Eyring fluid: Intelligent computing paradigm. *International Communications in Heat and Mass Transfer*. (129): 105683.
29. Ahmad, F., Gul, T., Khan, I., Saeed, A., Selim, M.M., Kumam, P., Ali, I. (2021). MHD thin film flow of the Oldroyd-B fluid together with bioconvection and activation energy. *Case Studies in Thermal Engineering*. (27): 101218.
30. Asif Zahoor Raja, M., Shoaib, M., Abbas, A., Ijaz Khan, M., Jagannatha, C.G., Gali, C., Malik, M.Y., Alwetaishi, M. (2022). Neuro-computing intelligent networks for entropy optimized MHD fully developed nanofluid flow with activation energy and slip effects. *Journal of the Indian Chemical Society*. (99): 100504.
31. Sharma, B.K., Sharma, P., Mishra, N. K., Fernandez-Gamiz, U. (2023). Darcy-Forchheimer hybrid nanofluid flow over the rotating Riga disk in the presence of chemical reaction: Artificial neural network approach. *Alexandria Engineering Journal*. (76): 101-130.
32. Alwani Salleh, S.N., Bachok, N., Arifin, N.M., Ali, F.M. (2020). Influence of Soret and Dufour on forced convection flow towards a moving thin needle considering Buongiorno's nanofluid model. *Alexandria Engineering Journal*. (59): 3897-3906.
33. Gopi Krishna, S., Shanmugapriya, M., Senthil Kumar, P. (2022). Prediction of bio-heat and mass transportation in radiative MHD Walter-B nanofluid using MANFIS model. *Mathematics and Computers in Simulation*. (201): 49-67.
34. Dalir, N., Dehsara, M., Nourazar, S. S. (2015). Entropy analysis for magnetohydrodynamic flow and heat transfer of a Jeffrey nanofluid over a stretching sheet. *Energy*. (79): 351-362.
35. Imtiaz, M., Hayat, T., Alsaedi, A. (2016). Flow of magneto nanofluid by a radiative exponentially stretching surface with dissipation effect. *Advanced Powder Technology*. (27): 2214-2222.
36. Daniel, Y.S., Abdul Aziz, Z., Ismail, Z., Salah, F. (2017) . Effects of thermal radiation, viscous and Joule heating on electrical MHD nanofluid with double stratification. *Chinese Journal of Physics*. (55): 630-651.
37. Abdul Gaffar, S., Ramachandra Prasad, V., Keshava Reddy, E. (2017). Computational study of Jeffrey's non-Newtonian fluid past a semi-infinite vertical plate with thermalradiation and heat generation/absorption. *Ain Shams Engineering Journal*. (8): 277-294.
38. Jain, S., kumari, M., Parmar, A. (2018). Unsteady MHD chemically reacting mixed convection nano-fluids flow past an inclined pours stretching sheet with slip effect and variable thermal radiation and heat source. *Materials Today: Proceedings*. (5): 6297-6312,
39. Krishna Prasad, D.V., Krishna Chaitanya, G.S., Srinivasa Raju, R. (2019). Double diffusive effects on mixed convection Casson fluid flow past a wavy inclined plate in presence of Darcian porous medium. *Results in Engineering*. (3): 100019.
40. Ijaz Khan, M., Alsaedi, A., Qayyum, S., Hayat, T., Imran Khan, M. (2019). Entropy generation optimization in flow of Prandtl-Eyring nanofluid with binary chemical reaction and Arrhenius

activation energy. *Colloids and Surfaces A*. (570): 117-126.

41. Haider, I., Nazir, U., Nawaz, M., Alharbi, S.O., Khan, I. (2021). Numerical thermal study on performance of hybrid nano-Williamson fluid with memory effects using novel heat flux model. *Case Studies in Thermal Engineering*. (26): 101070.
42. Dawar, A., Shah, Z., Islam, S., Deebani, W., Shutaywi, M. (2023). MHD stagnation point flow of a water-based copper nanofluid past a flat plate with solar radiation effect. *Journal of Petroleum Science and Engineering*. (220): 111148.
43. Awan, A.U., Ameer Ahammad, N., Majeed, S., Gamaoun, F., Ali, B. (2022). Significance of hybrid nanoparticles, Lorentz and Coriolis forces on the dynamics of water based flow. *International Communications in Heat and Mass Transfer*. (135): 106084.
44. Ali, K., Ahmad, S., Ahmad, S., Jamshed, W., Tirth, V., Algahtani, A., Al-Mughanam, T., Irshad, K., Alqahtani, H., M. El Din, S. (2023). Insights into the thermal attributes of sodium alginate (NaC6H7O6) based nanofluids in a three-dimensional rotating frame: A comparative case study. *Case Studies in Thermal Engineering*. (49): 103211.
45. Wang, F., Awais, M., Parveen, R., Alam, M.K., Rehman, S., Hassan deif, A. M., Shah, N. A. (2023). Melting rheology of three-dimensional Maxwell nanofluid (graphene-engine-oil) flow with slip condition past a stretching surface through Darcy-Forchheimer medium. *Results in Physics*. (51): 106647.
46. Wang, F., Tarakaramu, N., Sivakumar, N., Satya Narayana, P.V., Harish Babu, D., Ramalingam, S. (2023). Three dimensional nanofluid motion with convective boundary condition in presents of nonlinear thermal radiation via stretching sheet. *Journal of the Indian Chemical Society*. (100): 100887.
47. Majeed, A., Ijaz, N., Baazaoui, N., Barghout, K., Ali, S.S., Saleem, N., Hassan, A.M., Naeem, S. (2023). Enhanced thermal and mass transfer of harnessing microbial mediation in electrically conducting Oldroyed-B nanofluid flow: Eukaryotes microorganisms in biological applications. *Case Studies in Thermal Engineering*. 103570.
48. Ahmad, S., Ali, F., Khan, I., Haq, S. U. (2023). Biomedical applications of gold nanoparticles in thermofluids flow through a porous medium. *International Journal of Thermofluids*. (20): 100425.
49. Arshad, M. (2024). MHD hybrid nanofluid flow in a rotating system with an inclined magnetic field and thermal radiation. *Case Studies in Thermal Engineering* . (62): 105182.
50. Elayarani, M., Shanmugapriya, M., Senthil Kumar, P. (2021). Intensification of heat and mass transfer process in MHD carreau nanofluid flow containing gyrotactic microorganisms. *Chemical Engineering & Processing: Process Intensification*. (160): 108299.
51. Asif Zahoor Raja, M., Faizan Malik, M., Chang, C.L., Shoaib, C., Shu, M. (2021). Design of backpropagation networks for bioconvection model in transverse transportation of rheological fluid involving Lorentz force interaction and gyrotactic microorganisms. *Journal of the Taiwan Institute of Chemical Engineers*. (121): 276-291 .
52. Shoaib, M., Kausar, M., Nisar, K. S., Asif Zahoor Raja, M., Morsy, A. (2022). Impact of thermal energy on MHD Casson fluid through a Forchheimer porous medium with inclined non-linear surface: A soft computing approach. *Alexandria Engineering Journal*. (61): 12211-12228.
53. [53] Shafiq, A., Çolak, A.B., Sindhu, T.N. (2022). Significance of bioconvective flow of MHD thixotropic nanofluid passing through a vertical surface by machine learning algorithm. *Chinese Journal of Physics*. (80): 427-444.
54. Amna, Aljuaydi, F., Khan, Z., Islam, S. (2023). Numerical investigations of ion slip and hall effects on Cattaneo-Christov heat and mass fluxes in darcy-forchheimer flow of Casson fluid within a porous medium, utilizing non-fourier double diffusion theories through artificial neural networks ANNs. *International Journal of Thermofluids*. (20): 100475.
55. Kaswan, P., Kumar, M., Kumari, M. (2023). Analysis of a bioconvection flow of magnetocross nanofluid containing gyrotactic microorganisms with activation energy using an artificial neural network scheme. *Results in Engineering*. (17): 101015.
56. Butt, Z.I., Ahmad, I., Ilyas, H., Shoaib, M., Asif Zahoor Raja, M. (2023). Design of inverse multiquadric radial basis neural networks for the dynamical analysis of MHD casson nanofluid flow along a nonlinear stretchable porous surface with multiple slip conditions. *international journal o f hydrogen energy*. (48): 16100-16131.
57. Sabir, Z., Akkurt, N., Ben Said, S. (2023). A novel radial basis Bayesian regularization deep neural network for the Maxwell nanofluid applied on the Buongiorno model. *Arabian Journal of Chemistry*. (16): 104706.
58. Takhar, H.S., Chamkha, A.J., Nath, G. (2002). MHD flow over a moving plate in a rotating fluid with magnetic field, Hall currents and free stream velocity. *International Journal of Engineering Science*. (40): 1511-1527.